Floquet-Bloch Theory and Topology in Periodically Driven Lattices

A. Gómez-León and G. Platero

Instituto de Ciencia de Materiales de Madrid (ICMM-CSIC), Cantoblanco, 28049 Madrid, Spain

(Received 11 February 2013; published 14 May 2013)

We propose a general framework to solve tight binding models in D dimensional lattices driven by ac electric fields. Our method is valid for arbitrary driving regimes and allows us to obtain effective Hamiltonians for different external field configurations. We establish an equivalence with time-independent lattices in $D+1$ dimensions and analyze their topological properties. Furthermore, we demonstrate that nonadiabaticity drives a transition from topological invariants defined in $D+1$ to D dimensions. Our results have potential applications in topological states of matter and nonadiabatic topological quantum computation, predicting novel outcomes for future experiments.

DOI: 10.1103/PhysRevLett.110.200403 PACS numbers: 03.65.Vf, 03.65.Xp, 03.67.−a

Introduction.—Periodically driven quantum systems have been a fast-growing research field in recent years. The development of effective Hamiltonians describing ac-driven systems at certain regimes has allowed us to predict novel properties such as topological phases [1–5] and quantum phase transitions [6,7] that otherwise would be impossible to achieve in the undriven case. Therefore, the application of ac fields has become a very promising tool to engineer quantum systems. On the other hand, to obtain effective Hamiltonians can be a difficult task, depending on the driving regime to be considered.

In this Letter, we provide a general framework to study periodically driven quantum lattices. By means of our approach, it is possible to solve with arbitrary accuracy their time evolution and obtain effective Hamiltonians for the different driving regimes. We consider solutions of Floquet-Bloch form, based on the symmetries of the system, and characterize the states in terms of the quasienergies. As we will see below, it allows us to formally describe the ac-driven D dimensional lattice, as an analogue to a time-independent $D+1$ dimensional lattice. This description enlightens the underlaying structure of periodically driven systems, in which the initial Bloch band splits into several copies (Floquet-Bloch bands), where the coupling between them directly depends on the driving regime [8]. Interestingly, the isolated Floquet-Bloch bands possess the same topological properties as the Bloch bands of the undriven system, now tuned by the external field parameters. Thus, the topological invariants for the isolated Floquet-Bloch bands can be obtained following the general classification of time-independent systems [Altland-Zirnbauer (AZ) classes [9–11]]. However, we also demonstrate that on lowering the frequency, the bands couple to each other. In that case, the topological structures are classified according to a base manifold of dimension $D+1$.

Our approach is valid for arbitrary dimension, and it allows us to independently analyze the effect of the field amplitude and frequency. We show that the field amplitude controls the renormalization of the system parameters, while the frequency acts analogously to a dc electric field in the extra dimension. In particular, this last property relates the high-frequency regime with the existence of Bloch oscillations and Landau-Zener transitions between bands [12], establishing a direct relation between diabatic regime and localization [13]. We illustrate our formalism with the analysis of an ac-driven dimer chain [14–16].

Theory.—We consider a Hamiltonian with lattice and time translation invariance $H(\mathbf{x}+\mathbf{a}_i, t+T) = H(\mathbf{x}+\mathbf{a}_i, t) = H(\mathbf{x}, t+T)$, characterized by lattice vectors $\mathbf{a}_i$ and time period $T = 2\pi/\omega$. Under these assumptions, we use the Floquet-Bloch ansatz [17] $|\Psi_{\alpha,\mathbf{k}}(\mathbf{x}, t)\rangle = e^{i\mathbf{k}\cdot\mathbf{x}-i\epsilon_{\alpha,\mathbf{k}}t}|u_{\alpha,\mathbf{k}}(\mathbf{x}, t)\rangle$, with $\epsilon_{\alpha,\mathbf{k}}$ the quasi-energy for the Floquet state, α a band index, and $\mathbf{k}$ the wave vector. The Floquet-Bloch states $|u_{\alpha,\mathbf{k}}(\mathbf{x}, t)\rangle$ are periodic in both $\mathbf{x}$ and t and map the time-dependent Schrödinger equation to the eigenvalue equation in which t and $\mathbf{k}$ are both parameters,

$$\mathcal{H}(\mathbf{k}, t)|u_{\alpha,\mathbf{k}}\rangle = \epsilon_{\alpha,\mathbf{k}}|u_{\alpha,\mathbf{k}}\rangle, \tag{1}$$

$$\mathcal{H}(\mathbf{k}, t) \equiv e^{-i\mathbf{k}\cdot\mathbf{x}}(H(t) - i\partial_t)e^{i\mathbf{k}\cdot\mathbf{x}} = H_{\mathbf{k}}(t) - i\partial_t, \tag{2}$$

where $\mathcal{H}(\mathbf{k}, t)$ is the Floquet operator. Because of the time periodicity, the Floquet states can be expressed in terms of their Fourier components $|u_{\alpha,\mathbf{k},n}\rangle$. It allows one to consider the composed Hilbert space $\mathcal{S} = \mathcal{H} \otimes \mathcal{T}$ [18] for the basis $\{|u_{\alpha,\mathbf{k},n}\rangle\}$, where $\mathcal{T}$ is the space of T-periodic functions and $\mathcal{H}$ is the Hilbert space. We also introduce the composed scalar product $\langle\langle\cdots\rangle\rangle = \int_0^T\langle\cdots\rangle dt/T$, which gets rid of the time dependence. Finally, we define the Floquet-Bloch annihilation and creation operators $c(t)_{\alpha,\mathbf{k}}$, $c(t)^\dagger_{\alpha,\mathbf{k}}$, which satisfy

$$[c(t)^\dagger_{\alpha,\mathbf{k}}, c(t)_{\beta,\mathbf{k}'}]_\pm = \delta_{\mathbf{k},\mathbf{k}'}\delta_{\alpha,\beta}$$

for boson and fermions, respectively [19], where the time dependence of $c(t)_{\alpha,\mathbf{k}}$ is given by the time evolution operator. We propose below that an exact mapping between a

D dimensional ac-driven system and a $D+1$ undriven one can be established, in which $\mathcal{H}(\mathbf{k},t)$ is equivalent to a static Hamiltonian. It will allow us to classify the topological invariants in terms of the mappings from the parameter space to the set of Floquet operators $\mathcal{H}(\mathbf{k},t)$, being the parameter space now given by $S^1\times\mathbb{T}^n$, where n is the dimension of the first Brillouin zone (FBZ).

We first define the Fourier transforms

$$c(t)_{\alpha,\mathbf{k}}=N^{-D/2}\sum_{j=1}^{N}\sum_{n=-\infty}^{\infty}c_{\alpha,j,n}e^{-i\mathbf{k}\cdot\mathbf{R}_j+in\omega t},$$
$$c(t)^{\dagger}_{\alpha,\mathbf{k}}=N^{-D/2}\sum_{j=1}^{N}\sum_{n=-\infty}^{\infty}c^{\dagger}_{\alpha,j,n}e^{i\mathbf{k}\cdot\mathbf{R}_j-in\omega t}, \tag{3}$$

where N is the number of sites in the lattice with periodic boundary conditions and D is the dimension of the undriven system. For a time-dependent Hamiltonian in the dipolar approximation, the relation between undriven and driven system is given by the minimal coupling $\mathbf{k}\rightarrow\mathbf{K}(t)=\mathbf{k}+\mathbf{A}(t)$, where $\mathbf{A}(t)$ is the vector potential. Thus, one can obtain the time-dependent tight binding (TB) model by using the minimal coupling in the inverse Fourier transform, leading to the time-dependent hoppings $\tau(t)^{\alpha,\beta}_{j,l}=\tau^{\alpha,\beta}_{j,l}e^{i\mathbf{A}(t)\cdot(\mathbf{R}_j-\mathbf{R}_l)}$ and yielding the Hamiltonian

$$H_{\mathbf{k}}(t)=N^{-D}\sum_{\alpha,\mathbf{k}}\sum_{j,l}\tau(t)^{\alpha,\beta}_{j,l}e^{i\mathbf{k}\cdot(\mathbf{R}_j-\mathbf{R}_l)}c(t)^{\dagger}_{\beta,\mathbf{k}}c(t)_{\alpha,\mathbf{k}}, \tag{4}$$

where the time dependence in the operators is now included. Expansion in Fourier series $c(t)_{\alpha,\mathbf{k}}$ and $c(t)^{\dagger}_{\alpha,\mathbf{k}}$ [Eq. (3)] gives

$$H_{\mathbf{k}}(t)=N^{-D}\sum_{\alpha,\mathbf{k}}\sum_{n,m}\sum_{j,l}\tau(t)^{\alpha,\beta}_{j,l}c^{\dagger}_{\beta,\mathbf{k},n}c_{\alpha,\mathbf{k},m}e^{i\kappa(t)\cdot(\rho_{n,j}-\rho_{m,l})}, \tag{5}$$

with the quadrivectors $\kappa(t)\equiv(-t,\mathbf{k})$ and $\rho_{n,j}\equiv(n\omega,\mathbf{R}_j)$. Equation (5) gives a description of the time-dependent Hamiltonian in terms of the time-independent operators $\{c_{\alpha,\mathbf{k},n},c^{\dagger}_{\alpha,\mathbf{k},n}\}$. Finally, the use of the composed scalar product allows one to obtain the quasienergies by diagonalization of the matrix,

$$\langle\langle\mu_{\beta,k,n}|\mathcal{H}(\mathbf{k},t)|u_{\alpha,\mathbf{k},m}\rangle\rangle=\tilde{\tau}^{\alpha,\beta}_{n,m}-n\omega\delta_{n,m}\delta_{\alpha,\beta}, \tag{6}$$

$$\tilde{\tau}^{\alpha,\beta}_{n,m}\equiv\frac{1}{T}\int_0^T N^{-D}\sum_{j,l}^{N}\tau(t)^{\alpha,\beta}_{j,l}e^{i\kappa(t)\cdot(\rho n,j-\rho m,l)}dt, \tag{7}$$

where $n\omega\delta_{n,m}$ is the Fourier space representation of $-i\partial_t$. Equation (6) is analogous to a time-independent TB model in $D+1$ dimensions with an electric field of unit intensity applied along the extra dimension and sites labeled by (n,j) (see Fig. 1). The effective electric field breaks translational symmetry in the $\mathcal{E}$ axis, and one can differentiate two regimes of low and high frequency.

In the low-frequency regime ($\omega\ll\tau^{\alpha,\beta}_{j,i}$), it is a good approximation to neglect the effect of the time derivative in the Floquet operator [Eq. (2)], or equivalently, the Stark shift due to the effective electric field. Then, we restore the $\mathcal{E}$ axis translational symmetry, and the operator can be diagonalized by a Fourier transform of Eq. (6) to the t domain. The obtained $\mathcal{H}(\mathbf{k},t)$ is analogous to a Hamiltonian over a $D+1$ compact base manifold that we define as the first Floquet Brillouin zone (FFBZ), parametrized by $\{t,\mathbf{k}\}\in S^1\times\mathbb{T}^n$ (see the Supplemental Material [20]). Hence, the system topology is classified according to the AZ class of $D+1$ static Hamiltonians. Note that if one initially assumes adiabatic evolution, the Floquet structure, the parameters renormalization by the field amplitude, and the additional dimension of the base manifold are not obtained. Thus, the topological classification is not clearly established.

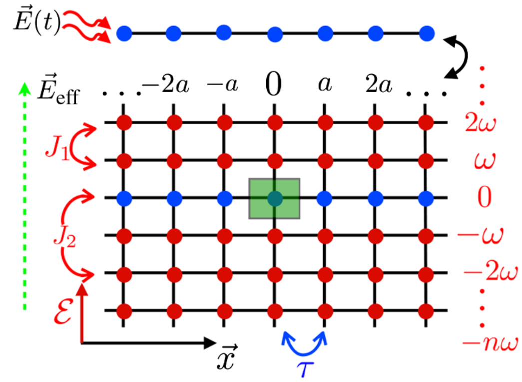

FIG. 1 (color online). Equivalence between a periodically driven 1D chain and the effective static lattice in 2D. The array of dots at $\mathcal{E}=0$ (blue) shows the positions of the undressed states at sites ra, $r\in\mathbb{Z}$. Each site is coupled to a set of dressed states (arrays of dots at $\mathcal{E}\neq0$, red color), with coupling $\propto\tau J_p(A_0)$, with $p=n-m$ the difference in the number of photons and A_0 the vector potential amplitude. We draw the Wigner-Seitz unit cell (green square) and the effective dc electric field (see text) along the energy axis $\mathcal{E}$ (green dotted arrow).

For high frequency ($\omega\gg\tau_{j,l}$), the effective electric field produces Bloch-Zener transitions and Bloch oscillations [12,13], inducing localization in $n\omega$, and decoupling the Floquet bands. Then, Eq. (6) becomes block diagonal in Fourier space and the effective Floquet operator time independent. In addition, it is defined over a D dimensional base manifold $\mathbf{k}\in\mathbb{T}^n$ (FBZ). In consequence, the topological classification is given by the AZ classes for time-independent systems in D dimensions. The transition from a $D+1$ to a D dimensional base manifold (equivalently, from the FFBZ to the FBZ), as one increases the frequency ω, is driven by the nonadiabatic processes along the t axis [21].

Importantly, note that in general the hopping between n, m neighbors depends on the amplitude of the vector potential [Eq. (7)]. It allows us to design "effective lattices" by tuning the hoppings with the ac field [22].

Periodically driven dimer chain.—Here, we consider a dimer chain coupled to an ac electric field, with hoppings τ

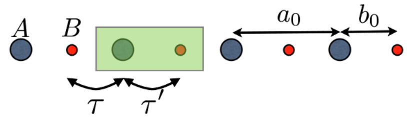

FIG. 2 (color online). Schematic figure for a dimer chain with two inequivalent atoms (A, B) for unit cell (green rectangle). b_0 is the intradimer distance, a_0 is the lattice translation vector, and τ' (τ) is the intra(inter) dimer hopping.

and τ', and periodic boundary conditions (Fig. 2). The electric field $E(t) = -\partial_t A(t)$ is given by the vector potential $A(t) = A_0 \sin(\omega t)$, where $A_0 \equiv qE_0/\omega$ (we fix $q = -1$).

From Eq. (7), one obtains in the basis of atom A/B

$$\tilde{\tau}^{\alpha,\beta}_{n,m} = \tau \begin{pmatrix} 0 & \rho_F(k) \\ \tilde{\rho}_F(k) & 0 \end{pmatrix},$$
$$\rho_F(k) \equiv \lambda e^{-ikb_0} J_{n-m}(A_0 b_0) + e^{ik(a_0-b_0)} J_{m-n}(A_0(a_0 - b_0)),$$
$$\tilde{\rho}_F(k) \equiv \lambda e^{ikb_0} J_{m-n}(A_0 b_0) + e^{-ik(a_0-b_0)} J_{n-m}(A_0(a_0 - b_0)), \tag{8}$$

where $\lambda = \tau'/\tau$, and $(n, m) \in \mathbb{Z}$. In contrast with the undriven case, the spectrum depends on the intradimer distance b_0, and the hoppings are renormalized by the field amplitude. Note that for the limit $A_0 \to 0$, the quasienergies match the energies of the undriven system.

We first consider the high-frequency regime ($\omega \gg \tau, \tau'$), where the Floquet operator is block diagonal and the system can be described by a time-independent 2×2 matrix

$$\mathcal{H}^{(0)}_k = \tau \vec{g}(k) \cdot \vec{\sigma}, \tag{9}$$

where $\vec{g}(k) = (\Re(\tilde{\rho}_F), \Im(\tilde{\rho}_F), 0)$ for $n = m = 0$, and $\vec{\sigma} = (\sigma_x, \sigma_y, \sigma_z)$ are the Pauli matrices. Figure 3 shows the quasienergy spectrum in high-frequency regime. We include in green dotted lines the regions of existence of edge states, obtained from the numerical calculation of the

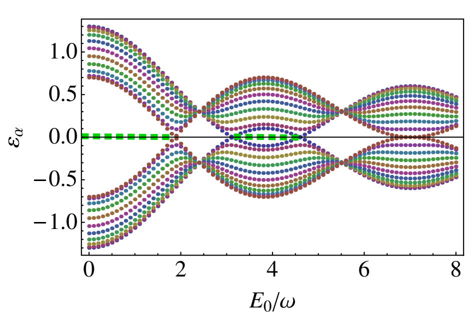

FIG. 3 (color online). Quasienergy spectrum vs E_0/ω for $\lambda = 0.3$ and $b_0 = 0$, considering Eq. (9) (high frequency). The band structure is obtained by considering 10 k vectors equally spaced within the FBZ. We also included in green dashed lines the gapless modes obtained from the numerical calculation ($\omega = 10\tau$).

finite size system with Hamiltonian $H(t) = H_0 + qE(t)x$, with H_0 the time-independent TB Hamiltonian and $qE(t)x$ the coupling with the electric field (details in the Supplemental Material [20]). The appearance of zero energy modes is a finite size effect linked to the underlying topology of the system. The bulk to edge correspondence relates the number of zero energy modes at the boundary, carrying a topological number, with the bulk topological invariants [23]. Therefore, the calculation of the topological invariants of $\mathcal{H}^{(0)}_k$ should predict their existence in this regime (Fig. 3). $\mathcal{H}^{(0)}_k$ belongs to the chiral orthogonal class (BDI) class (as the one corresponding to the undriven system), with time reversal, particle-hole, and chiral symmetry [11]. In one dimension (1D), the BDI class is characterized by a winding number ν_1, which classifies mappings $\mathbb{T}^1 \to \mathbb{R}^2 - \{0\} \simeq S^1$, from the FBZ to the family of Hamiltonians $\mathcal{H}^{(0)}_k$

$$\nu_1 = \oint \langle u_{\alpha,k} | i\partial_k | u_{\alpha,k} \rangle dk$$
$$= \frac{\pi}{2}[1 + \mathrm{sgn}(J_0^2(y) - \lambda^2 J_0^2(x))], \tag{10}$$

where $y \equiv A_0(a_0 - b_0)$, $x \equiv A_0 b_0$, and $|u_{\alpha,k}\rangle$ are the closed lifts of $\mathcal{H}^{(0)}_k$. Equation (10) shows that in contrast with the undriven case [14], one can create nontrivial topological phases even for $\lambda > 1$, where the undriven system is in the trivial phase (Fig. 4 left). This is an example of topology induced by the driving.

In Fig. 4 (right), we plot the phase diagram for $\lambda = 0.3$, which correctly predicts the existence of edge states for $b_0 = 0$ (Fig. 3). In summary, we have shown that in the high-frequency regime, the topological properties can be obtained using an effective static Hamiltonian $\mathcal{H}^{(0)}_k$ and that they can be tuned by the field amplitude.

As we decrease ω, the different Floquet bands couple to each other, and the isolated band picture is not accurate. In

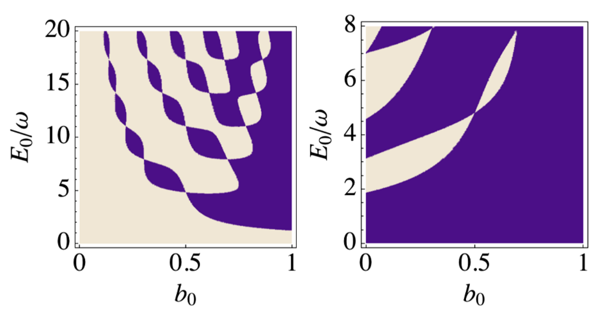

FIG. 4 (color online). Topological phase diagram at high frequency for an ac-driven dimer chain with $\lambda = 1.5$ (left) and $\lambda = 0.3$ (right). Dark shading: $\nu_1 = \pi$, and light shading: $\nu_1 = 0$. Note that even for $\lambda > 1$ we can induce a nontrivial topology, in contrast with the undriven case. Furthermore, the phase diagram for $\lambda = 0.3$ (right) agrees with the existence of the edge states in Fig. 3 ($b_0 = 0$).

this regime, one must consider the full Floquet operator [Eq. (1)], which for this system is not exactly solvable. Because of the coupling between Floquet bands, two different but related effects happen as ω is reduced: band inversions, and the emergence of a $D+1$ parameter space.

Band inversions correspond to crossings of the bands, in which the symmetry is exchanged (e.g., it occurs in quantum wells of HgTe/CdTe as the well thickness reaches a critical value [23]). This effect happens in ac-driven systems as we decrease the frequency, because the distance between Floquet bands is proportional to ω. If the maximum width of an isolated Floquet band is given by $\delta\epsilon \leq \omega$ ($\epsilon_\alpha \in [-\omega/2, \omega/2]$), the Floquet bands at $\pm\omega$ close the gap when $\omega = \delta\epsilon/2$. As a general rule, band inversions happen for every

$$\omega_n = \frac{\delta\epsilon}{2n}, \qquad n \in \mathbb{Z}^+, \tag{11}$$

where $\mathbb{Z}^+$ denotes the set of positive integers. Therefore, at ω_n the $\pm n\omega$ Floquet bands close the gap, switching between an ordinary and a topological insulating phase. For example, for a dimer chain with $b_0 = 0$, the maximum width coincides with the undriven system band width $\delta\epsilon = \delta E = 2\tau\sqrt{1+\lambda^2+2\lambda}$. Then, it is possible to track the bands inversions in terms of the undriven system (see the Supplemental Material [20]).

For $\omega \ll \tau$, τ', a large number of bands inversions occur, and it is difficult to track all of them. In addition, the presence of a $D+1$ base manifold becomes important. In that case, one can neglect the time derivative in Eq. (2) and diagonalize the operator in the t domain. In that case, one obtains a 2×2 Floquet operator $\mathcal{H}(k,t) \simeq H(k,t)_{\rm NNN}$ defined over the FFBZ, where $H(k,t)_{\rm NNN}$ extends up to next-nearest neighbors coupling in (n, m) (it is a good approximation for $A_0 \leq 1$). However, two-dimensional (2D) Hamiltonians in the BDI class are topologically trivial, and only the 1D topological invariant ν_1 is still nonzero. It means that all changes in the topological properties will be reflected in ν_1. In addition, for BDI Hamiltonians, one can compute the winding number graphically [14], in terms of the divergences of the phase $\phi(k,t) = \arctan(g_y/g_x)$ over the FFBZ (Fig. 5), with $g_{x,y}$ the components of the vector

$$H(k,t)_{\rm NNN} = \tau\vec{g}(k,t)\cdot\vec{\sigma}. \tag{12}$$

Note that in difference with Eq. (9), $\vec{g}(k,t)$ now depends on t, and ν_1 can be defined along the two inequivalent axes of the torus

$$\nu_1(\eta) = \frac{1}{2}\oint \frac{\partial}{\partial\mu}\phi(\mu,\eta)d\mu, \qquad \mu, \eta = k, t.$$

For the case of a finite chain, the existence of boundary states depends on the loops along the k axis, i.e., on $\nu_1(t)$ [14]. In Fig. 5, $\nu_1(t) = \pi$ for all t values, independent of the value of E_0/ω (trajectories always cross two discontinuities).

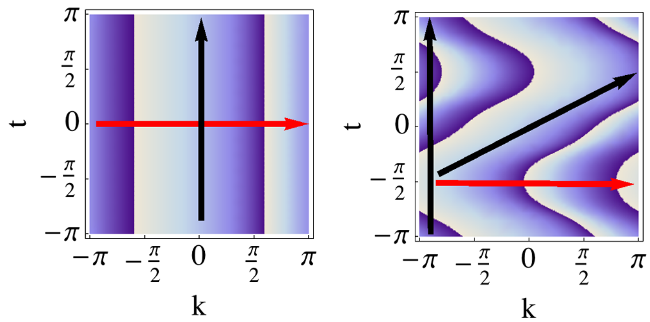

FIG. 5 (color online). Plot of $\phi(k,t)$ all over the FFBZ for $A_0 = 0$ (left) and $A_0 = 2$ (right). Paths parallel to k cross two discontinuities meaning $\nu_1 = \pi$ (red horizontal arrows), and on the other hand, paths parallel to t, or those which do not cross a discontinuity, have $\nu_1 = 0$ because they wind back and forth (black arrows).

Thus, gap inversions are not relevant for the existence of edge states at low frequency, being a feature of the transition from the FBZ to the FFBZ. This can be seen numerically in the finite size system, in which zero energy modes are present independently on the gap inversions (see the Supplemental Material [20]).

Conclusions.—We have derived a general approach to solve periodically driven D dimensional lattices. It allows us to obtain effective Hamiltonians for the different driving regimes and a complete topological classification in terms of AZ classes. We show that even for high frequency, the underlying topology of the undriven system is present due to the time periodicity. In addition, we show that for low frequency, the Floquet operator is analogous to the one of a static system in $D+1$ dimensions, leading to interesting topological states of matter which otherwise would be inaccessible. Finally, we also described the mechanism of band inversion in ac-driven systems and its relation with the topology of the system.

For the dimer chain, we have obtained exact expressions in Fourier space for the quasienergies, without invoking a low-energy approximation, which accounts for both the lattice and field symmetries. It allows us to obtain the effective Hamiltonian at low frequency, which in difference with the one in high frequency, presents boundary states for a wide range of field amplitudes. In addition, the simplicity of the system and its relation with other systems such as graphene [14] motivates the study of it. We expect that ac-driven superconducting systems in 1D would be interesting to study due to their change in the topological invariant from 1D to 2D. Also, the present results can be useful for the cold atoms and quantum dots communities as well as for nonadiabatic topological quantum computation.

Finally, we have shown a large horizon of possibilities for periodically driven systems, which in addition, can be studied experimentally, e.g., by measuring the electric polarizability [13] or the appearance of boundary states. The driving allows us to simulate properties of undriven systems in higher dimensions and the obtention of new topological phases due to tunable hoppings [22]. One could also think of more exotic types of zero energy modes in the low-frequency regime, for example, those in the boundary between driven and undriven materials. Also, further studies in the case of bichromatic ac fields could be interesting.

We thank P. Delplace, A. G. Grushin, S. Kohler, P. C. E. Stamp, and M. Büttiker for useful discussions. A. G. L. acknowledges the JAE program (MICINN) and we both acknowledge Grant No. MAT2011-24331 and the ITN Grant No. 234970 (EU).

[1] J. I. Inoue and A. Tanaka, Phys. Rev. Lett. **105**, 017401 (2010).
[2] N. Lindner, G. Refael, and V. Galitski, Nat. Phys. **7**, 490 (2011).
[3] L. Jiang, T. Kitagawa, J. Alicea, A. R. Akhmerov, D. Pekker, G. Refael, J. Ignacio Cirac, E. Demler, M. D. Lukin, and P. Zoller, Phys. Rev. Lett. **106**, 220402 (2011).
[4] M. Busl, G. Platero, and A.-P. Jauho, Phys. Rev. B **85**, 155449 (2012).
[5] Z. Gu, H. A. Fertig, D. P. Arovas, and A. Auerbach, Phys. Rev. Lett. **107**, 216601 (2011).
[6] V. M. Bastidas, C. Emary, B. Regler, and T. Brandes, Phys. Rev. Lett. **108**, 043003 (2012).
[7] V. M. Bastidas, C. Emary, G. Schaller, and T. Brandes, Phys. Rev. A **86**, 063627 (2012).
[8] P. Delplace, A. Gómez-León, and G. Platero, arXiv:1304.6272.
[9] M. R. Zirnbauer, J. Math. Phys. (N.Y.) **37**, 4986 (1996).
[10] A. Altland and M. R. Zirnbauer, Phys. Rev. B **55**, 1142 (1997).
[11] A. P. Schnyder, S. Ryu, A. Furusaki, and A. W. W. Ludwig, Phys. Rev. B **78**, 195125 (2008).
[12] C. Zener, Proc. R. Soc. A **145**, 523 (1934).
[13] N. Marzari, A. Mostofi, J. Yates, I. Souza, and D. Vanderbilt, Rev. Mod. Phys. **84**, 1419 (2012).
[14] P. Delplace, D. Ullmo, and G. Montambaux, Phys. Rev. B **84**, 195452 (2011).
[15] W. P. Su, J. R. Schrieffer, and A. J. Heeger, Phys. Rev. Lett. **42**, 1698 (1979).
[16] S. Ryu and Y. Hatsugai, Phys. Rev. Lett. **89**, 077002 (2002).
[17] G. Platero and R. Aguado, Phys. Rep. **395**, 1 (2004).
[18] H. Sambe, Phys. Rev. A **7**, 2203 (1973).
[19] M. Grifoni and P. Hänggi, Phys. Rep. **304**, 229 (1998).
[20] See the Supplemental Material at http://link.aps.org/supplemental/10.1103/PhysRevLett.110.200403 for details of the relation between the driven and undriven Hamiltonian, and a detailed analysis of the driven dimer chain.
[21] A. Gómez-León and G. Platero, Phys. Rev. B **86**, 115318 (2012).
[22] W. Beugeling, J. C. Everts, and C. Morais Smith, Phys. Rev. B **86**, 195129 (2012).
[23] M. Hasan and C. Kane, Rev. Mod. Phys. **82**, 3045 (2010).